The Influence of Processing Parameters on the Tensile Strength of 3D Printed Products

Van-Long Trinh
School of Mechanical and Automotive Engineering, Hanoi University of Industry, Hanoi, Vietnam
longtv@haui.edu.vn (corresponding author)

Tien-Dung Hoang
School of Mechanical and Automotive Engineering, Hanoi University of Industry, Hanoi, Vietnam
tiendunghaui@gmail.com

Quang-Tu Ngo
School of Mechanical and Automotive Engineering, Hanoi University of Industry, Hanoi, Vietnam
tunq@haui.edu.vn

Received: 14 February 2025 | Revised: 3 March 2025 | Accepted: 9 March 2025

 DOI: https://doi.org/10.48084/etasr.10573

ABSTRACT

Additive Manufacturing (AM) is a modern method of producing parts by depositing material layers on each other. The technology can be used to fabricate many different types of products for daily applications. Tensile Strength (TS) is one of the most important mechanical properties of fabricated products, such as 3D-printed products. This study investigates the influence of Additive Manufacturing Parameters (AMPs) on the TS of manufactured products. 3D printed samples were produced using Fused Deposition Modeling (FDM) technology with Polylactic Acid (PLA) material. The AMPs investigated were temperature, speed, layer thickness, and bed temperature. TS tests were carried out on a tensile testing machine, and the results showed that AMPs have a great influence on TS. In addition, the optimal set of AMPs was found for the manufacturing process to improve TS. TS can be predicted using a response model obtained from response optimization analysis. The results of this study can be applied in various practical applications.

Keywords-additive manufacturing; processing parameters; FDM; PLA

I. INTRODUCTION

3D printing or Additive Manufacturing (AM) technology has made significant advances in manufacturing science and technology [1-4]. AM technology creates products with high precision and minimum waste of raw materials, without subtractive manufacturing techniques [5]. AM shows outstanding advantages in the production of thin, complex, and multi-material structure products [6-8]. AM is widely applied in many fields, such as manufacturing [9], construction [10, 11], automobile [12], biology [13-16], medical [17], soft robotics [18], orthognathic surgery [19], food industry [20-22], medicine [23], electronics [24], liver surgery [25], dentistry [26], fashion [27], and aerospace [28]. Fused Deposition Modeling (FDM) is a popular AM technology using polymer materials and composite filaments. FDM shows good characteristics such as versatility, cost-effectiveness, diversity, and non-toxicity of materials.

However, the FDM technology still needs to be extensively studied to improve the durability and mechanical properties of products such as Tensile Strength (TS). TS is one of the most important mechanical properties of fabricated products [29]. Polylactic Acid (PLA) is becoming popular and is widely applied in AM for practical applications. PLA is an easy-to-process polymer. PLA 3D printing products can serve many applications, such as household products, decorations, household items, small furniture parts, medical models, medical instruments, and medical prosthetics, due to their safety and ease of sterilization [30]. Many studies seek methods and techniques to improve the characteristics of the 3D printed products such as the effect of processing factors on TS with printing angle [31], thickness of the printing layers [32], printing temperature [33], or using artificial neural networks to optimize mechanical properties [34] and finite element analysis to enhance the stiffness of the 3D printed gears.

However, there is still a lack of studies on TS and AM fabrication conditions. This study investigates the influence of 3D printing parameters on the TS of printed products, using FDM with PLA. The AM Parameters (AMPs) include the printing temperature, speed, thickness of the printing layer, and bed temperature. TS tests were carried out to determine the effect of AMPs on TS. In addition, TS was predicted using a regression model from response optimization analysis.

II. EXPERIMENT PROCEDURE

PLA was used to fabricate the 3D products for the experiments. This material is suitable for many applications such as industrial manufacturing, educating models, and medicine applications. PLA has good characteristics of easy printing, high precision, and low deformation during the printing process. Table I shows the basic mechanical properties and reference printing parameters of PLA [35].

TABLE I. BASIC MECHANICAL PROPERTIES AND REFERENCE PRINTING PARAMETERS OF PLA

Property	Typical value
Nozzle temperature	185-205°C
Heat bed temperature	55-60°C
Melting point	175-180°C
Softening temperature	50°C
Elastic modulus	3.5 GPa
Glass transition temperature	60-65°C
Density	1.23-1.25 g/cm³

The 3D printer used for the experiments is an ANYCUBIC I3 Mega S 3D of the well-known Prusa series with the basic specifications shown in Table II [36]. Figure 1 shows images of AM samples that were modeled using NX software with detailed dimensions. The tensile test samples adhere to ASTM D638 [37].

TABLE II. BASIC SPECIFICATIONS OF THE ANYCUBIC I3 MEGA S 3D PRINTER

Technical specifications	Values
Nozzle diameter	0.4 mm
Printing Speed	20 ~ 100 mm/s
Printing temperature	Maximum 260ºC
Bed temperature	Maximum 110ºC

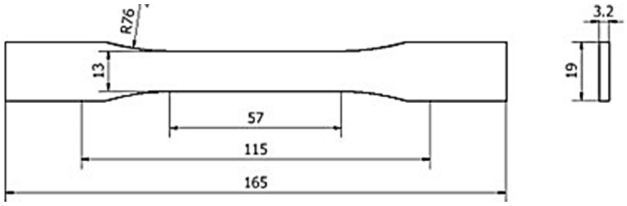

Fig. 1. Images of the 3D printing samples with detailed dimensions, including the bottom view on the left and the side view on the right.

Table III shows the Box-Behnken experimental matrix with processing parameters used to analyze the impact of AMPs on the TS of the product including the printing temperature (*Tp*), speed (*V*), layer thickness (*h*), and bed temperature (*Tb*). The input parameters were set to three values according to three levels: -1, 0, and 1. Figure 2 shows the BESTUTM 050MD Universal Compression/Tensile Testing Machine that was used to perform the tensile test.

TABLE III. PROCESS PARAMETERS AND THEIR LEVELS

Parameters	Unit	Symbol	Levels		
			-1	0	1
Temperature	℃	*Tp*	190	210	230
Printing speed	mm/s	*V*	40	60	80
Thickness of the printing layer	mm	*h*	0.1	0.2	0.3
Bed temperature	℃	*Tb*	30	45	60

Fig. 2. BESTUTM 050MD Universal Compression/Tensile Testing Machine.

TABLE IV. EXPERIMENTAL DESIGN AND RESULTS

Run	*Tp* (℃)	*V* (mm/s)	*h* (mm)	*Tb* (℃)	*TS* (kN/mm²)
1	210	60	0.2	45	0.046
2	210	40	0.2	30	0.049
3	210	80	0.3	45	0.045
4	190	60	0.2	30	0.045
5	210	60	0.3	30	0.042
6	210	60	0.1	30	0.037
7	190	60	0.2	60	0.035
8	210	40	0.2	60	0.046
9	190	60	0.3	45	0.043
10	230	80	0.2	45	0.043
11	190	40	0.2	45	0.044
12	210	60	0.2	45	0.044
13	210	80	0.2	60	0.046
14	230	60	0.2	60	0.045
15	210	60	0.2	45	0.044
16	230	60	0.1	45	0.045
17	230	40	0.2	45	0.048
18	210	40	0.3	45	0.045
19	190	60	0.1	45	0.040
20	210	60	0.3	60	0.041
21	210	80	0.1	45	0.039
22	210	80	0.2	30	0.040
23	230	60	0.2	30	0.042
24	210	60	0.1	60	0.043
25	230	60	0.3	45	0.043
26	190	80	0.2	45	0.042
27	210	40	0.1	45	0.043

III. RESULTS AND DISCUSSION

Figure 3 shows the specimens after the TS tests. Table IV shows the experimental results of 27 specimens, with the highest strength of 0.049 kN/mm^2. Analysis was carried out using Minitab software with the significance level chosen as 0.05 ($\alpha = 0.05$).

Fig. 3. Specimens after TS tests.

Figure 4 shows the main effects of AMPs on the TS of the samples. Figure 4(a) shows the effect of *Tp* on TS, indicating that TS gradually increases as the nozzle temperature increases. This may be due to the improvement in interlayer adhesion when the temperature was high enough for the PLA material layers to fuse better. However, at higher temperatures there was no obvious decrease, indicating that this temperature range (from 190°C to 230°C) is suitable for maintaining adhesion without damaging the material. Figure 4(b) shows the effect of *V* on TS, indicating that TS tends to decrease as *V* increases. At high V, the time it takes for the new material layer to bond to the previous printed layer is short, leading to a decrease in interlayer adhesion and resulting in a lower TS. At slower *V* values, there is an improvement in the bonding process, resulting in patterns with higher TS. Figure 4(c) shows the effect of *h* on TS, indicating that increasing *h* resulted in a decrease in TS. This may be because in thicker layers, the adhesion between them reduces as a result of poor material mixing. Thinner layers improve TS because they are better bonded, and the gaps between them are reduced. Figure 4(d) shows the effect of *Tb* on TS. As *Tb* increases, TS increases. A higher *Tb* improves the adhesion of the resin layer to the substrate, leading to a reduction in warping or delamination of the samples.

Figure 5 shows the interaction relationships of the AMPs that affect the TS of the product. Figure 5(a) shows the interaction effect of *Tp* and *V* on TS. TS increases sharply with increasing nozzle temperature, especially at low print speeds. Figure 5(b) shows the interaction effect of *Tp* and *h* on TS. At the *h* of 0.1 mm, the nozzle temperature increases, and the TS increases sharply. However, at thicker layers, increasing nozzle temperature does not bring about a significant improvement in TS. Figure 5(c) shows the interaction effect of *V* and *h* on the TS, indicating that both *V* and *h* play an important role in TS. Figure 5(d) shows the interaction effect of the *Tp* and *Tb* on TS. The *Tp* and *Tb* interaction has the most significant influence on TS. This is a reason to focus on the processing parameters of controlling the TS of the product. Figure 5(e) shows the interaction effect of the *V* and the *Tb* on TS, where at low *V* and high *Tb*, TS reaches the maximum value. Figure 5(f) shows the interaction effect of the *h* and *Tb* on TS. The interaction of *h* and *Tb* influences TS, indicating that the combination of these factors also needs to be carefully considered to achieve the best results.

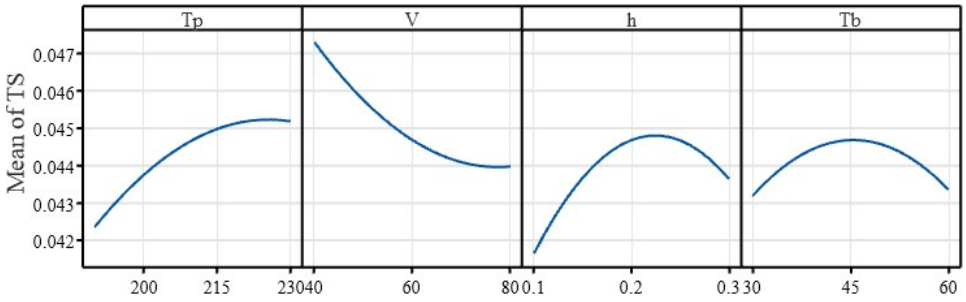

Fig. 4. Main effects for TS: (a) The effect of printing temperature on TS, (b) The effect of printing speed on TS, (c) The effect of printing layer thickness on TS, (d) The effect of the bed temperature on TS.

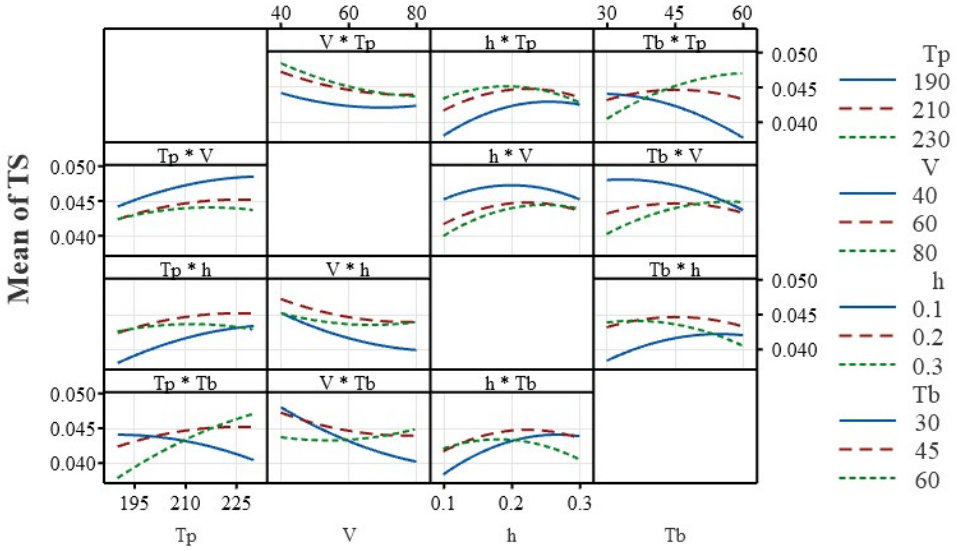

Fig. 5. Interaction effects of printing parameters on TS: (a) Temperature and speed, (b) Temperature and layer thickness, (c) Speed and layer thickness, (d) Temperature and bed temperature, (e) Speed and bed temperature, (f) Layer thickness and bed temperature.

Figure 6 shows the Pareto chart of the effects of AMPs on TS. This chart shows that *Tp* has the highest effect on TS with the effect value above the normalization threshold of 2.179 as analyzed by Minitab. *V* stands in the second position of the effects, followed by *h* and *Tb* at the final position. The chart also shows the interaction effects of the AMPs on TS, with the highest effect being the combination of *Tp* and *Tb*. The combined effect of *V* and *Tb* is in the second position during the printing process. The following combinations of AMPs, in descending order, include the couples of *h* and *Tb*, *Tp* and *h*, *V* and *h*, and *Tp* and *V*. Figure 7 shows the response surface regression of TS with *Tp*, *V*, *h*, and *Tb*.

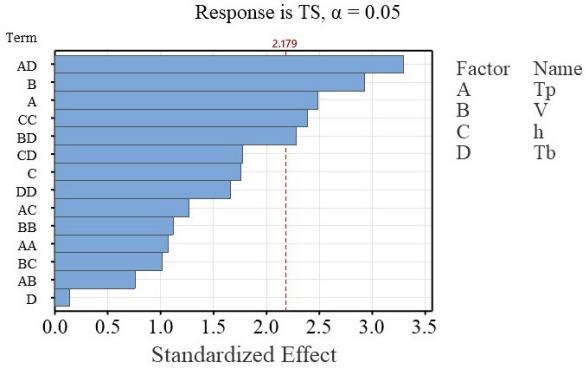

Fig. 6. Pareto chart of the standardized effects for TS.

A TS regression equation was formulated from the experimental data [38]:

$$TS = -0.013 + 0.000783\,Tp - 0.000415\,V + 0.245\,h - 0.001919\,Tb - 0.000002\,Tp*Tp + 0.000002\,V*V - 0.2042\,h*h - 0.000006\,Tb*Tb - 0.000002\,Tp*V - 0.000625\,Tp*h + 0.000011\,Tp*Tb + 0.000500\,V*h + 0.000008\,V*Tb - 0.001167\,h*Tb \quad (1)$$

Coded Coefficients

Term	Coef	SE Coef	T-Value	P-Value	VIF
Constant	0.04467	0.00114	39.20	0.000	
Tp	0.001417	0.000570	2.49	0.029	1.00
V	-0.001667	0.000570	-2.93	0.013	1.00
h	0.001000	0.000570	1.76	0.105	1.00
Tb	0.000083	0.000570	0.15	0.886	1.00
Tp*Tp	-0.000917	0.000855	-1.07	0.305	1.25
V*V	0.000958	0.000855	1.12	0.284	1.25
h*h	-0.002042	0.000855	-2.39	0.034	1.25
Tb*Tb	-0.001417	0.000855	-1.66	0.123	1.25
Tp*V	-0.000750	0.000987	-0.76	0.462	1.00
Tp*h	-0.001250	0.000987	-1.27	0.229	1.00
Tp*Tb	0.003250	0.000987	3.29	0.006	1.00
V*h	0.001000	0.000987	1.01	0.331	1.00
V*Tb	0.002250	0.000987	2.28	0.042	1.00
h*Tb	-0.001750	0.000987	-1.77	0.102	1.00

Model Summary

S	R-sq	R-sq(adj)	R-sq(pred)
0.0019738	81.40%	59.71%	0.00%

Fig. 7. Response surface regression: TS versus *Tp*, *V*, *h*, and *Tb*.

The regression model has R^2 of 81.40% and R^2(adj) of 59.71%, respectively. R^2 is used to evaluate the accuracy of the regression model. The correction coefficient R^2(adj) shows that the change in TS is determined by the change in input parameters at the level of 59.71%. Figure 8 shows the results of the response optimization analysis. The objective is to investigate the AMP set for the maximum value of TS. The results show that this function can achieve a maximum TS of approximately 0.0493 kN/mm². This optimal TS is higher than the values of the tests after 27 experiments, with the maximum value of 0.049 kN/mm² recorded from experiment no. 2 (see the experimental design table). The optimal printing parameter set included a printing temperature of 190°C, a printing speed of 40 mm/s, a printing layer thickness of 0.2737 mm, and a bed temperature of 30°C, as shown in Table V.

TABLE V. OPTIMIZATION PARAMETERS FOR THE 3D-PRINTING PROCESS OF PLA MATERIAL

Tp (°C)	*V* (mm/s)	*h* (mm)	*Tb* (°C)	*TS* (kN/mm²)
190	40	0.2737	30	0.0493

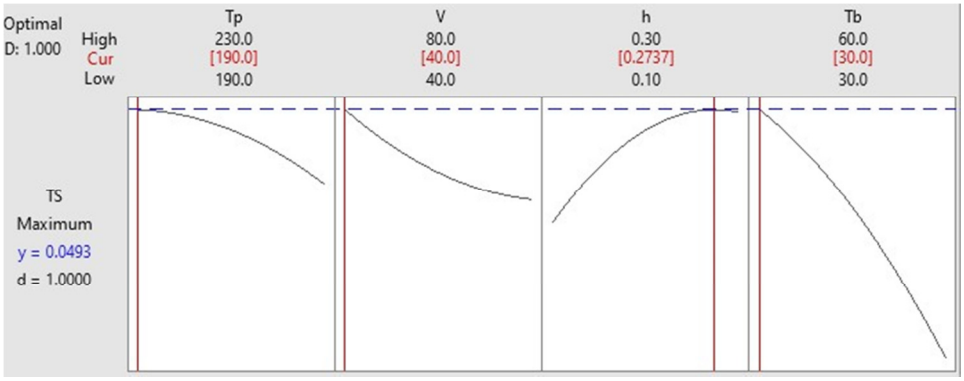

Fig. 8. Response optimization analysis of processing parameters on TS.

IV. CONCLUSIONS

AM is a modern manufacturing technology to produce parts by depositing material layer by layer, used to create products for daily applications. TS is an important mechanical property of products such as 3D printing samples. This study investigated the influence of AMPs on the TS of 3D-printed products. The results show that the printing speed has the greatest influence on TS, followed by the printing temperature, the thickness of the printing layer, and the bed temperature, respectively. The optimal parameters set was built for the AM process to improve TS. The response model was built using response optimization analysis to predict the TS. The results of this study can be applied in various practical applications.

ACKNOWLEDGMENT

This work was sponsored by the Hanoi University of Industry, Vietnam.

REFERENCES

[1] Z. Zhang, B. Wang, D. Hui, J. Qiu, and S. Wang, "3D bioprinting of soft materials-based regenerative vascular structures and tissues," *Composites Part B: Engineering*, vol. 123, pp. 279–291, Aug. 2017, https://doi.org/10.1016/j.compositesb.2017.05.011.

[2] X. Wang, M. Jiang, Z. Zhou, J. Gou, and D. Hui, "3D printing of polymer matrix composites: A review and prospective," *Composites Part B: Engineering*, vol. 110, pp. 442–458, Feb. 2017, https://doi.org/10.1016/j.compositesb.2016.11.034.

[3] T. D. Ngo, A. Kashani, G. Imbalzano, K. T. Q. Nguyen, and D. Hui, "Additive manufacturing (3D printing): A review of materials, methods, applications and challenges," *Composites Part B: Engineering*, vol. 143, pp. 172–196, Jun. 2018, https://doi.org/10.1016/j.compositesb.2018.02.012.

[4] P. Parandoush and D. Lin, "A review on additive manufacturing of polymer-fiber composites," *Composite Structures*, vol. 182, pp. 36–53, Dec. 2017, https://doi.org/10.1016/j.compstruct.2017.08.088.

[5] D. I. Wimpenny, P. M. Pandey, and L. J. Kumar, Eds., *Advances in 3D Printing & Additive Manufacturing Technologies*. Springer, 2017.

[6] A. A. Stepashkin, D. I. Chukov, F. S. Senatov, A. I. Salimon, A. M. Korsunsky, and S. D. Kaloshkin, "3D-printed PEEK-carbon fiber (CF) composites: Structure and thermal properties," *Composites Science and Technology*, vol. 164, pp. 319–326, Aug. 2018, https://doi.org/10.1016/j.compscitech.2018.05.032.

[7] L. Pyl, K. A. Kalteremidou, and D. Van Hemelrijck, "Exploration of the design freedom of 3D printed continuous fibre-reinforced polymers in open-hole tensile strength tests," *Composites Science and Technology*, vol. 171, pp. 135–151, Feb. 2019, https://doi.org/10.1016/j.compscitech.2018.12.021.

[8] H. L. Tekinalp *et al.*, "Highly oriented carbon fiber–polymer composites via additive manufacturing," *Composites Science and Technology*, vol. 105, pp. 144–150, Dec. 2014, https://doi.org/10.1016/j.compscitech.2014.10.009.

[9] B. Berman, "3-D printing: The new industrial revolution," *Business Horizons*, vol. 55, no. 2, pp. 155–162, Mar. 2012, https://doi.org/10.1016/j.bushor.2011.11.003.

[10] R. J. M. Wolfs, F. P. Bos, and T. A. M. Salet, "Early age mechanical behaviour of 3D printed concrete: Numerical modelling and experimental testing," *Cement and Concrete Research*, vol. 106, pp. 103–116, Apr. 2018, https://doi.org/10.1016/j.cemconres.2018.02.001.

[11] B. Panda, J. H. Lim, and M. J. Tan, "Mechanical properties and deformation behaviour of early age concrete in the context of digital construction," *Composites Part B: Engineering*, vol. 165, pp. 563–571, May 2019, https://doi.org/10.1016/j.compositesb.2019.02.040.

[12] M. R. Talagani *et al.*, "Numerical simulation of big area additive manufacturing (3D printing) of a full size car," *SAMPE Journal*, vol. 51, no. 4, pp. 27–36, Jul. 2015.

[13] J. Li *et al.*, "Flexible Organic Tribotronic Transistor Memory for a Visible and Wearable Touch Monitoring System," *Advanced materials (Deerfield Beach, Fla.)*, vol. 28, no. 1, pp. 106–110, Jan. 2016, https://doi.org/10.1002/adma.201504424.

[14] J. Chen *et al.*, "Automatic Mode Transition Enabled Robust Triboelectric Nanogenerators," *ACS Nano*, vol. 9, no. 12, pp. 12334–12343, Dec. 2015, https://doi.org/10.1021/acsnano.5b05618.

[15] A. Blaeser, D. F. Duarte Campos, U. Puster, W. Richtering, M. M. Stevens, and H. Fischer, "Controlling Shear Stress in 3D Bioprinting is a Key Factor to Balance Printing Resolution and Stem Cell Integrity," *Advanced Healthcare Materials*, vol. 5, no. 3, pp. 326–333, 2016, https://doi.org/10.1002/adhm.201500677.

[16] W. Zhu, X. Ma, M. Gou, D. Mei, K. Zhang, and S. Chen, "3D printing of functional biomaterials for tissue engineering," *Current Opinion in Biotechnology*, vol. 40, pp. 103–112, Aug. 2016, https://doi.org/10.1016/j.copbio.2016.03.014.

[17] Q. Yan *et al.*, "A Review of 3D Printing Technology for Medical Applications," *Engineering*, vol. 4, no. 5, pp. 729–742, Oct. 2018, https://doi.org/10.1016/j.eng.2018.07.021.

[18] J. Z. Gul *et al.*, "3D printing for soft robotics – a review," *Science and Technology of Advanced Materials*, vol. 19, no. 1, pp. 243–262, Dec. 2018, https://doi.org/10.1080/14686996.2018.1431862.

[19] H. H. Lin, D. Lonic, and L. J. Lo, "3D printing in orthognathic surgery – A literature review," *Journal of the Formosan Medical Association*, vol. 117, no. 7, pp. 547–558, Jul. 2018, https://doi.org/10.1016/j.jfma.2018.01.008.

[20] J. I. Lipton, M. Cutler, F. Nigl, D. Cohen, and H. Lipson, "Additive manufacturing for the food industry," *Trends in Food Science & Technology*, vol. 43, no. 1, pp. 114–123, May 2015, https://doi.org/10.1016/j.tifs.2015.02.004.

[21] J. Sun, W. Zhou, D. Huang, J. Y. H. Fuh, and G. S. Hong, "An Overview of 3D Printing Technologies for Food Fabrication," *Food and Bioprocess Technology*, vol. 8, no. 8, pp. 1605–1615, Aug. 2015, https://doi.org/10.1007/s11947-015-1528-6.

[22] F. C. Godoi, S. Prakash, and B. R. Bhandari, "3d printing technologies applied for food design: Status and prospects," *Journal of Food Engineering*, vol. 179, pp. 44–54, Jun. 2016, https://doi.org/10.1016/j.jfoodeng.2016.01.025.

[23] C. Dong, M. Petrovic, and I. J. Davies, "Applications of 3D printing in medicine: A review," *Annals of 3D Printed Medicine*, vol. 14, May 2024, Art. no. 100149, https://doi.org/10.1016/j.stlm.2024.100149.

[24] G. L. Goh, H. Zhang, T. H. Chong, and W. Y. Yeong, "3D Printing of Multilayered and Multimaterial Electronics: A Review," *Advanced Electronic Materials*, vol. 7, no. 10, 2021, Art. no. 2100445, https://doi.org/10.1002/aelm.202100445.

[25] J. S. Witowski *et al.*, "3D Printing in Liver Surgery: A Systematic Review," *Telemedicine and e-Health*, vol. 23, no. 12, pp. 943–947, Dec. 2017, https://doi.org/10.1089/tmj.2017.0049.

[26] L. Lin, Y. Fang, Y. Liao, G. Chen, C. Gao, and P. Zhu, "3D Printing and Digital Processing Techniques in Dentistry: A Review of Literature," *Advanced Engineering Materials*, vol. 21, no. 6, 2019, Art. no. 1801013, https://doi.org/10.1002/adem.201801013.

[27] C. K. Jeong *et al.*, "Topographically-Designed Triboelectric Nanogenerator via Block Copolymer Self-Assembly," *Nano Letters*, vol. 14, no. 12, pp. 7031–7038, Dec. 2014, https://doi.org/10.1021/nl503402c.

[28] D. W. Martinez, M. T. Espino, H. M. Cascolan, J. L. Crisostomo, and J. R. C. Dizon, "A Comprehensive Review on the Application of 3D Printing in the Aerospace Industry," *Key Engineering Materials*, vol. 913, pp. 27–34, 2022, https://doi.org/10.4028/p-94a9zb.

[29] N. G. Tanikella, B. Wittbrodt, and J. M. Pearce, "Tensile strength of commercial polymer materials for fused filament fabrication 3D printing," *Additive Manufacturing*, vol. 15, pp. 40–47, May 2017, https://doi.org/10.1016/j.addma.2017.03.005.

[30] D. G. Zisopol, I. Nae, A. I. Portoaca, and I. Ramadan, "A Statistical Approach of the Flexural Strength of PLA and ABS 3D Printed Parts," *Engineering, Technology & Applied Science Research*, vol. 12, no. 2, pp. 8248–8252, Apr. 2022, https://doi.org/10.48084/etasr.4739.

[31] J. Kiendl and C. Gao, "Controlling toughness and strength of FDM 3D-printed PLA components through the raster layup," *Composites Part B: Engineering*, vol. 180, Jan. 2020, Art. no. 107562, https://doi.org/10.1016/j.compositesb.2019.107562.

[32] T. Yao, J. Ye, Z. Deng, K. Zhang, Y. Ma, and H. Ouyang, "Tensile failure strength and separation angle of FDM 3D printing PLA material: Experimental and theoretical analyses," *Composites Part B: Engineering*, vol. 188, May 2020, Art. no. 107894, https://doi.org/10.1016/j.compositesb.2020.107894.

[33] M. H. Hsueh *et al.*, "Effect of Printing Parameters on the Thermal and Mechanical Properties of 3D-Printed PLA and PETG, Using Fused Deposition Modeling," *Polymers*, vol. 13, no. 11, Jan. 2021, Art. no. 1758, https://doi.org/10.3390/polym13111758.

[34] S. Subramonian *et al.*, "Artificial Neural Network Performance Modeling and Evaluation of Additive Manufacturing 3D Printed Parts," *Engineering, Technology & Applied Science Research*, vol. 13, no. 5, pp. 11677–11684, Oct. 2023, https://doi.org/10.48084/etasr.6185.

[35] "PETG Filament," *Kingroon 3D*. https://kingroon.com/collections/petg-filament.

[36] "Anycubic i3 Mega S" https://store.anycubic.com/products/anycubic-i3-mega-s.

[37] D20 Committee, "Test Method for Tensile Properties of Plastics." ASTM International, https://doi.org/10.1520/D0638-14.

[38] A. Dean and D. Voss, Eds., "Fractional Factorial Experiments," in *Design and Analysis of Experiments*, Springer, 1999, pp. 483–545.